Generating thickness gradients of thin polymer films via flow coating

Christopher M. Stafford,[a] Kristen E. Roskov, Thomas H. Epps III, and Michael J. Fasolka
Polymers Division, National Institute of Standards and Technology, Gaithersburg, Maryland 20899

(Received 25 November 2005; accepted 15 January 2006; published online 24 February 2006)

Thickness is a governing factor in the behavior of films and coatings. To enable the high-throughput analysis of this parameter in polymer systems, we detail the design and operation of a "flow coater" device for fabricating continuous libraries of polymer film thickness over tailored ranges. Focusing on the production of model polystyrene film libraries, we thoroughly outline the performance of flow coating by varying critical factors including device geometry, device motion, and polymer solution parameters. [DOI: 10.1063/1.2173072]

I. INTRODUCTION

The advent of combinatorial and high-throughput techniques for drug discovery,[1] and more recently for materials science,[2] has illuminated the power of these methods for accelerating product discovery and functional knowledge generation. Combinatorial and high-throughput methodologies depend upon the ability to fabricate specimen *libraries* that systematically survey parameters of interest over wide ranges. For materials science, this entails producing libraries that spatially vary factors governing performance and behavior, such as composition and processing parameters. There are two main paradigms for materials library design and fabrication. *Discrete* libraries consist of a collection of distinct subspecimens arranged in an orderly array. Discrete libraries offer wide surveys of large parameter spaces, but fabrication of these arrays often involves an extensive robotics infrastructure. In contrast, *gradient* libraries (considered in this work) exhibit a gradual and continuous change in one or more parameters as a function of position. By their nature, gradient specimens have a limited scope; however, such libraries offer an unparalleled means for thoroughly mapping material behavior over a specific range of parameter space and for exactly identifying critical phenomenon such as phase boundaries. Moreover, as discussed below, gradient libraries can be produced with a modest investment in equipment.

Beginning with the seminal work of Hanak,[3] materials researchers from several groups have introduced methods for fabricating continuous gradients in a variety of parameters, such as composition,[4,5] temperature,[6,7] surface energy,[7,8] and UV exposure.[9] In concert with this growing body of research, this article considers a method for creating continuous gradient libraries in polymer film thickness. In the context of a combinatorial workflow, steep gradients provide a broad survey of a phenomenon or process over a large parameter space while shallow gradients offer access to finer details and higher resolution measurements. Our apparatus, which we have termed a "flow coater," has been demonstrated in previous work from our group and others. These former studies applied the device to map the effect of film thickness on phenomena such as wetting,[10,11] block copolymer morphology,[12,13] and crazing/fracture.[14,15] In the current article, we detail the design and operation of our flow coater. In particular, we provide an extensive set of data that demonstrates the performance of the instrument over a variety of critical factors including device geometry, device motion, and polymer solution parameters.

II. DEVICE CONCEPTS

Flow coating is ideal for generating gradients in polymer film thickness in the submicron regime. The apparatus, illustrated in Fig. 1, consists of a stationary knife blade fixed at some distance (gap height) above a movable stage. Typical gap heights range from tens of microns to hundreds of microns. The substrate to be coated is rigidly fixed to the stage, and a bead of polymer solution is deposited/wicked between the blade and the substrate. The blade is then accelerated with respect to the substrate. The flow coating process draws upon a competition between (1) capillary forces holding the polymer solution between the stationary knife blade and the substrate, and (2) frictional drag exerted on that same solution as the blade is pulled across the substrate. Flow coating is similar in concept to other metered flows such as dip coating and blade coating. Readers are referred to several review articles[16,17] for details and further references on the various types of coating flows. However, an exact fluid mechanics model that best represents the flow dynamics encountered in our process has yet to be developed, and we are currently generating an appropriate theoretical model to predict the flow coating behavior documented in this work.

In flow coating, capillary forces hold the polymer solution under the blade at the initial condition of zero velocity; over time, the volume will slowly decrease due to evaporation of solvent from the edges. At low velocities, capillary forces still aim to keep the material between the substrate and the blade, but frictional drag causes some solution to escape under the knife blade. This material is left behind in the form of a wet film, which then dries by solvent evaporation. At higher velocities, the frictional drag increases and

[a]Author to whom correspondence should be addressed; electronic mail: chris.stafford@nist.gov

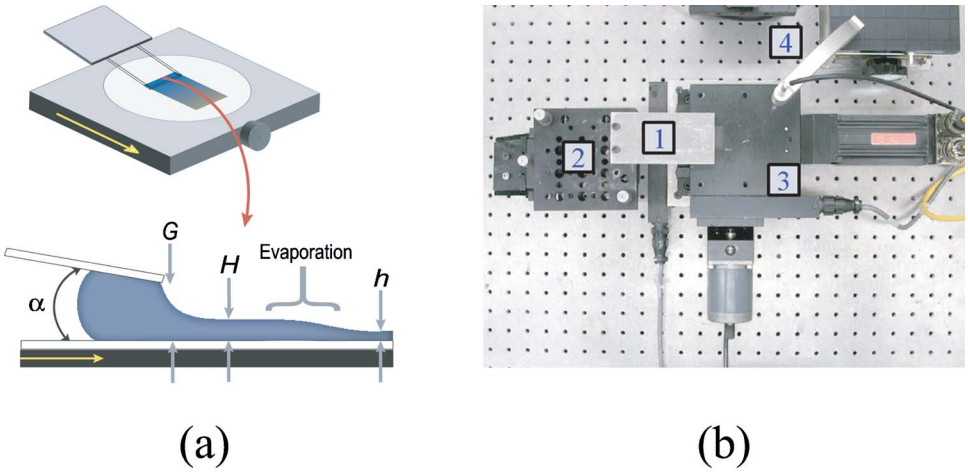

FIG. 1. (Color online) (a) Schematic of the flow coating process for generating thin films of uniform or gradient thickness, where α is the blade angle, G is the height of the blade above the substrate, H is the thickness of the wet film, and h is the dry film thickness. The substrate is moving in the direction of the arrow. (b) Aerial view of the NCMC flow coater: (1) stationary knife blade (glass slide) attached to an aluminum support, (2) tip-tilt-rotation-height stage assembly, (3) motorized x-y stage assembly, and (4) spot interferometer system.

more solution is deposited on the substrate in the form of a film. Thus, the instantaneous velocity controls the amount of the polymer solution left behind.

To better illustrate the concept of flow coating, two representative cases are presented in Fig. 2. Mode I consists of a plateaued velocity profile with a maximum acceleration (a) and deceleration (ad) of the stage. The result of this mode is a uniform film with a thickness dictated by the plateau velocity (v) and a length (d_f) controlled by the total distance of travel (less the short distance required to accelerate and decelerate the stage). Mode II consists of a ramped velocity profile with a constant acceleration and a maximum deceleration. In this case, the acceleration (more specifically, the instantaneous velocity at any given location) controls the resulting thickness of the film. The result of this mode is a film with a gradient in thickness, where the stage acceleration dictates the steepness of the gradient and the total distance traveled controls the range of thickness. These two cases are not meant to be inclusive, but rather demonstrate avenues of conventional use; more complex acceleration and velocity profiles that yield more complex thickness contours can certainly be realized with this instrument.

III. EXPERIMENTAL SETUP AND OPERATION

A. Design of gradient flow coater

Here we describe the design and construction of our flow coating instrument. Certain dimensions, such as the range of travel of translation stages, were chosen to suit our research goals but could be adapted to accommodate larger film dimensions with minor adjustments and appropriate calibration.

The flow coating apparatus is displayed in Fig. 1(b). The principle component of the system is the stationary knife blade (1) that is positioned above the substrate to be coated (not shown). The knife blade is held in place by a three-axis tip-tilt-rotation stage mounted on a z-axis (height) stage (2),[18] allowing the user to precisely and independently adjust the blade tilt (roll), blade angle (pitch), and the perpendicularism of the blade edge to the axis of motion (yaw). The z-axis stage permits adjustment of the blade height. All adjustments are made via micrometers. The substrate is rigidly mounted on a motorized x-y stage (3).[19] The flow coater itself only requires the x axis of motion for accelerating the substrate underneath the knife blade. However, we employ the x-y capability to map the thickness of the resulting film using a spot interferometer (4) (see Sec. III D).

We have experimented with several knife blades ranging from a simple putty knife (roughness typical of stamped steel) commercially available from a hardware store to a cleaved silicon wafer (atomically smooth break along a crystal plane) mounted at the end of an aluminum plate. The current blade of choice is a standard glass microscope slide with dimensions of either 25×75 mm^2 or 50×75 mm^2 fixed to an aluminum plate. The glass slide has several advantages:

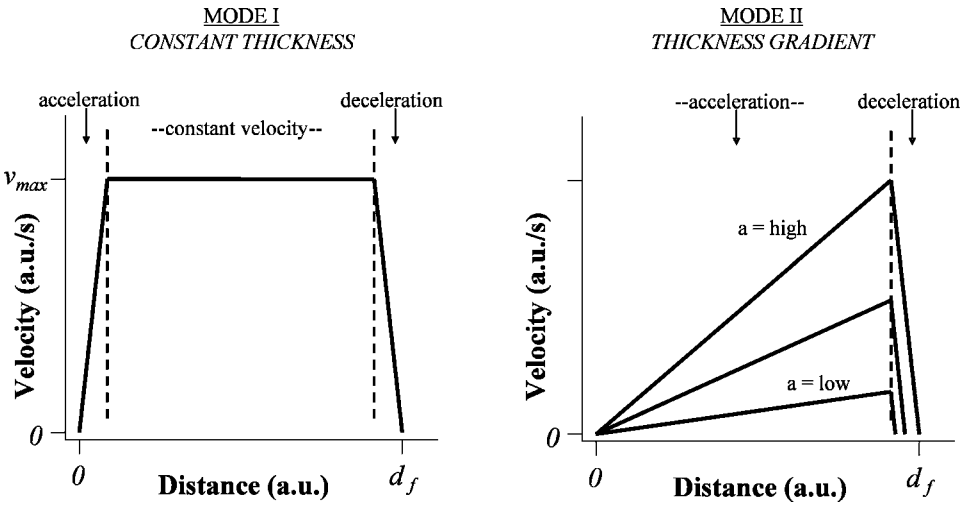

FIG. 2. Schematic of two simple operation modes for the flow coating apparatus. Mode I produces a film with a constant thickness as a function of distance, while mode II produces a film possessing a thickness gradient.

typical glass slides are fairly smooth; they are optically transparent, thus allowing visualization of the bead of solution that will be deposited under the knife blade; and they are inexpensive and disposable. The width of the knife blade (and thus the width of the final polymer film) can be varied from 25 to 50 to 75 mm, depending on which edge of the glass slide is oriented along the axis of acceleration. We have machined grooves in the aluminum plate to allow for precise and repeatable placement of the glass blade with respect to the substrate and axis of motion.

B. Sample preparation

Substrates for flow coating can be any flat surface such as polished silicon wafers or glass slides, depending on the acceptable surface roughness of the substrate. Silicon wafers have one distinct advantage in that thin polymer films show distinct interference colors upon reflection of light that are indicators of film thickness; therefore, through quick visual inspection, a user can ascertain the approximate thickness range and defect character of the newly generated film. Appropriate measures should be taken to ensure the substrate is clean of adsorbed organic contaminants. The substrates should be coated immediately after cleaning/drying to minimize adsorption of contaminants, and the knife blade should also be cleaned just prior to coating. Dilute polymer solutions are prepared by dissolving the polymer of interest in an appropriate volatile organic solvent (e.g., toluene). Typical concentrations are in the range of 0.1 to 10 wt % polymer. As in spin coating, all polymer solutions should be filtered prior to flow coating to prevent dust or other particulates from marring the final film.

C. Operation

The flow coating apparatus is operated through a computer interface which sends commands to the stage via a stand-alone motion controller. Using our custom-designed computer interface panel, the user can assign values to four operational parameters: acceleration (a), velocity (v), distance traveled (d_f), and deceleration (ad). The user can also adjust two geometrical parameters prior to coating: the gap height between the blade and substrate (G) and volume of solution dispensed (V). There are several other geometrical and physical parameters that can be adjusted (e.g., blade angle, surface energy of the blade and substrate), but these will not be discussed in detail here.

Recall that the local thickness of the film is controlled by the instantaneous velocity $[v(t)]$ of the blade with respect to the substrate and that lower velocities generate thinner films. Therefore, a low acceleration will result in a relatively shallow thickness gradient, and a high acceleration will result in a relatively steep gradient (for mode II operation). The motion controller determines when to commence deceleration based on a calculation of the distance required to bring the stage to a halt at the user-defined deceleration. Thus, if the acceleration and deceleration are assigned the same value, the thickness gradient will be symmetric (increasing and decreasing with the same slope) centered on $d_f/2$.

A typical procedure for generating a thickness gradient via flow coating is outlined as follows. The substrate is rigidly affixed to the translation stage; adhesive tape is sufficient. A knife blade is mounted on the tip-tilt-rotation stage. The blade is positioned at a fixed angle ($\alpha \approx 5°$ in our system) and brought down into contact with the substrate. At this point, the blade tilt is adjusted to bring the blade level with the surface of the substrate. The blade is then elevated to a given height (G) above the substrate (typically 200 μm), and a bead of polymer solution (typically $V \approx 50$ μL for a 25-mm-wide blade) is syringed along the leading edge of the blade. Since the blade height is only a couple hundred micrometers, capillary forces wick and hold the solution under the blade. Once the solution is placed under the knife blade, the operational commands are sent to the translation stage to initiate the desired motion $(a, v_{\max}, d_f, ad)$. As the stage moves, a liquid film remains behind, the thickness of which is influenced by a number of factors discussed earlier. The liquid film then dries to a solid film whose thickness is determined by the solids concentration in the wet film.

D. Mapping the thickness profile

In our instrument, the thickness at positions along the library is determined using a UV-visible interferometer (Model F20, Filmetrics, Inc.) operated in reflectance mode

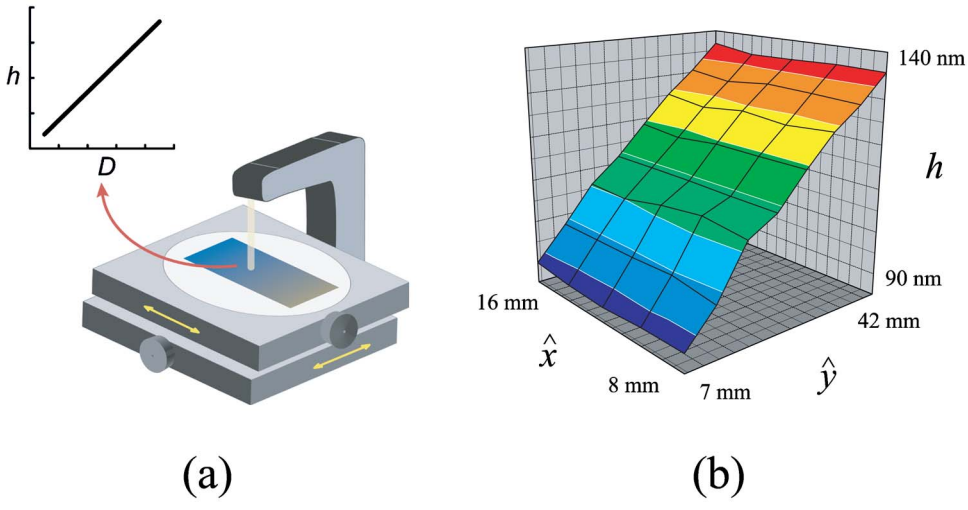

FIG. 3. (Color online) (a) Schematic of the x-y translation stage assembly and interferometry tool for generating film thickness maps, and (b) a representative three-dimensional (3D) thickness map generated using our flow coater/interferometer assembly.

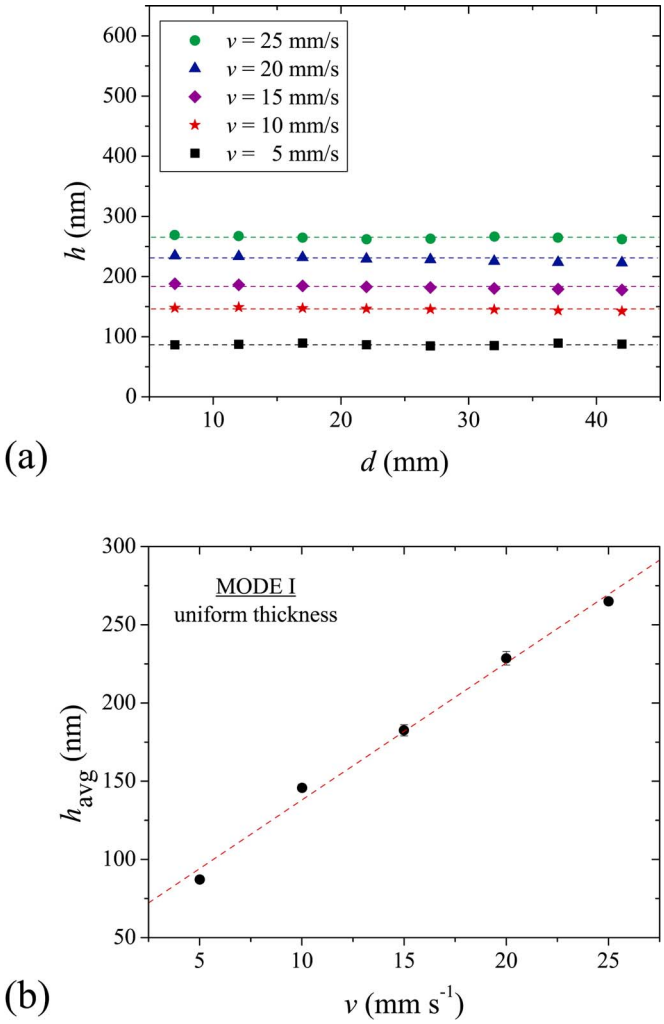

FIG. 4. (Color online) (a) Examples of mode I (uniform thickness) as a function of velocity (v) for 4.75 wt % 50k PS in toluene using $G=200$ μm and $V=50$ μL, and (b) the average film thickness (h_{avg}) as a function of velocity. The dashed lines are linear fits to the data. Most error bars are smaller than the symbols.

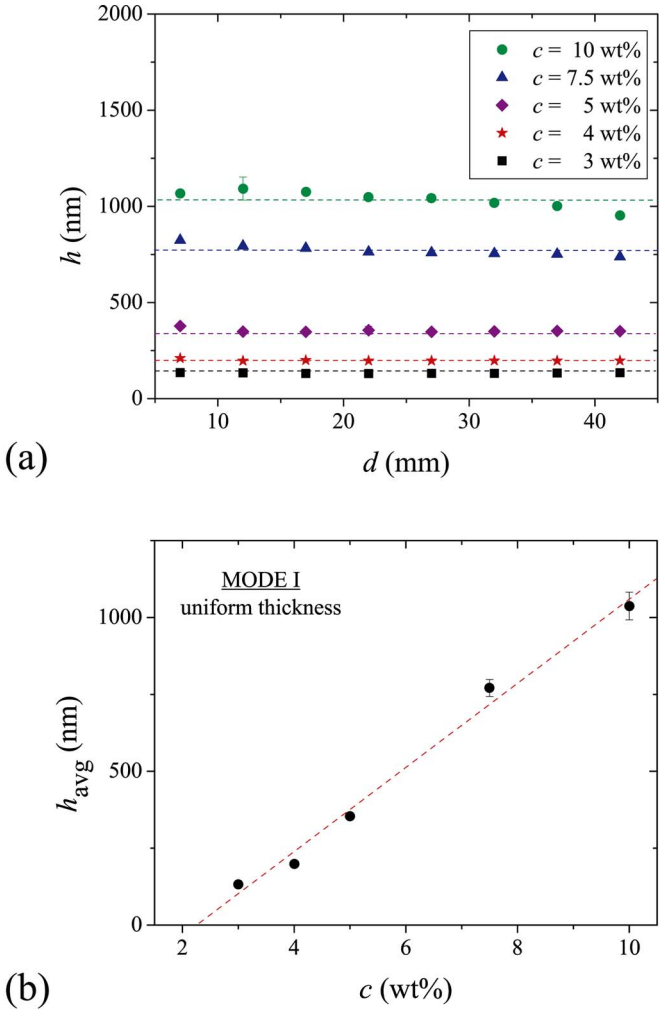

FIG. 5. (Color online) (a) Dependence of films of uniform thickness (mode I) on solution concentration (c) for 50k PS in toluene using $v=25$ mm s^{-1}, $G=200$ μm, and $V=50$ μL, and (b) the average film thickness (h_{avg}) as a function of solution concentration. The dashed lines are linear fits to the data. Most error bars are smaller than the symbols.

with a spot size of ≈0.5 mm and an acquisition time of a few seconds. To generate thickness maps, we employ the x-y translation stage assembly to raster the film under the interferometer and acquire thickness data as a function of position [see Fig. 3(a)]. A simple automation routine, written in PYTHON programming language, coordinates the stage motion, data acquisition, and data storage. In a typical routine, data are acquired over a 5×10 grid ($\hat{x}\times\hat{y}$, where $\hat{y}$ is the axis of the thickness gradient) with a spacing of 2 mm in $\hat{x}$ and 5 mm in $\hat{y}$. These data can be plotted as a contour plot for visualization, as shown in Fig. 3(b). Alternatively, the data can be averaged along $\hat{x}$ (constant thickness) for each step in $\hat{y}$; this method is used in the examples discussed in this manuscript.

IV. RESULTS

Based on our experiments, we have identified four (4) key factors in the flow coating process: instantaneous velocity, solution concentration, blade height, and bead volume. These four factors will be highlighted in this article. This is not meant to be a comprehensive list, and we continue to assess the effects of various other geometrical and solution properties on the flow coating process. Ultimately, the measurable in our flow coating experiments is the film thickness (h), measured by interferometry, as a function of distance along the coating direction (d). For all experiments described here, the polymer investigated was a poly(styrene) (PS) standard with a molecular mass of 50 000 g/mol and polydispersity of 1.04 (Polymer Source, Inc.).[20] We will use a shorthand notation of 50k PS throughout this manuscript.

Examples of mode I operation (uniform film thickness) can be seen in Fig. 4.[21] In these experiments, we used a 4.75 wt % solution of 50k PS in toluene, a blade height of $G=200$ μm, and a solution volume of $V=50$ μL. Acceleration and deceleration of the stage occur over the first and last few millimeters, and data from these transient regions are eliminated from the graphs. The film thickness remains uniform along the length of the film, with deviations in thickness of less than 2% across the film. As shown in Fig. 4(b), the film thickness exhibits a linear dependence on stage velocity, with thicker films correlating to increased velocity. Alternately, the film thickness can be adjusted by changing

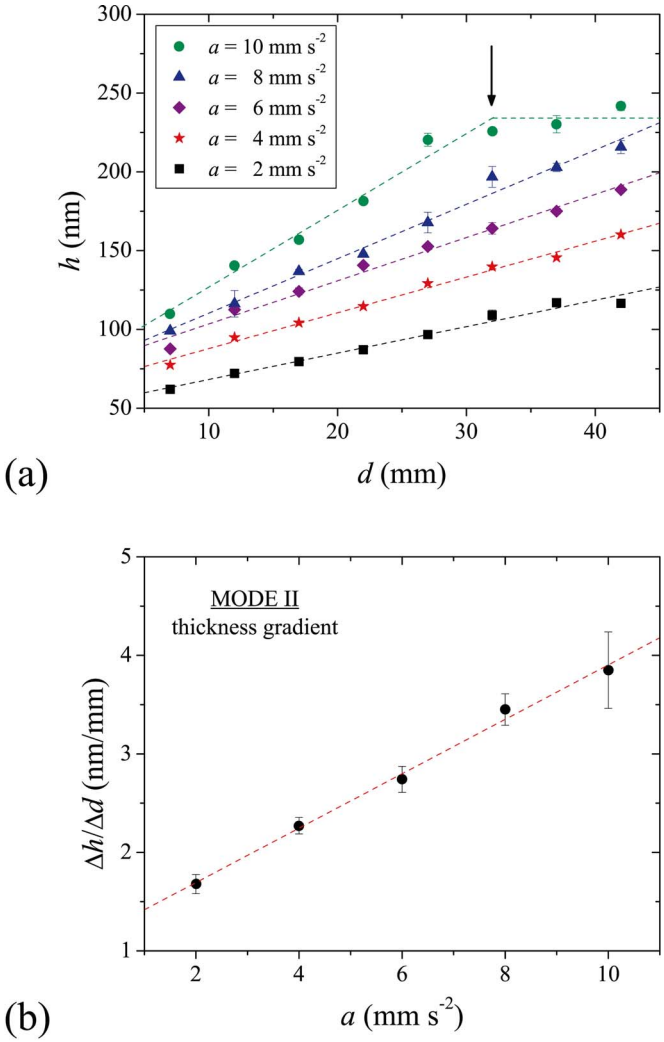

FIG. 6. (Color online) (a) Examples of mode II (thickness gradient) as a function of acceleration (a) for 4 wt % 50k PS in toluene using $G=200$ μm and $V=50$ μL, and (b) the slope of the gradient ($\Delta h/\Delta d$) as a function of acceleration. At $a=10$ mm s^{-2}, the stage reaches maximum velocity at $d=32$ mm (indicated by the arrow) and as a result the film thickness reaches a plateau. The dashed lines are linear fits to the data. Most error bars are smaller than the symbols.

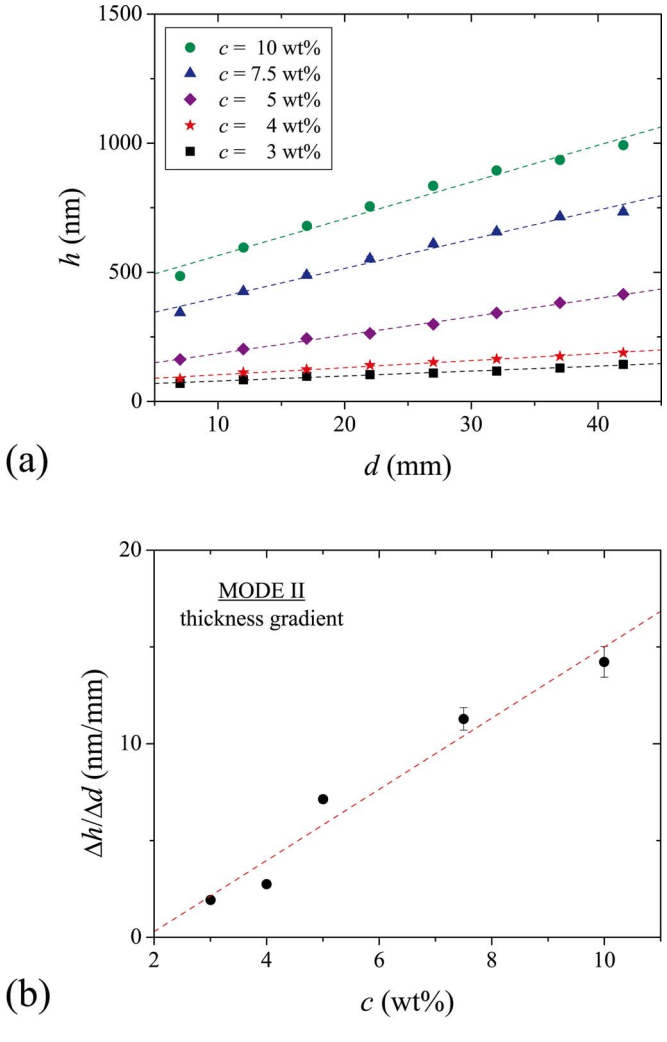

FIG. 7. (Color online) (a) Dependence of the film thickness gradient (h vs d) on solution concentration (c) for 50k PS in toluene using $a=6$ mm s^{-2}, $G=200$ μm, and $V=50$ μL, and (b) the slope of the gradient ($\Delta h/\Delta d$) as a function of solution concentration. The dashed lines are linear fits to the data. Most error bars are smaller than the symbols.

the solution concentration, as shown in Fig. 5. For this example, we chose the stage velocity to be the highest value attainable by our system ($v=25$ mm s^{-1}) to illustrate the maximum range of film thicknesses achievable under these settings. The film thickness also exhibits a reasonably linear dependence on solution concentration, as shown in Fig. 5(b). The observed thickness range spans an order of magnitude from sub-100 nm to several microns. In our experience, flow coating becomes more difficult with more concentrated solutions ($c>10$ wt %). If one needs thicker films, traditional doctor blade or metering rod coating is advised.

Films with a gradient in film thickness are fabricated using mode II operation, where the instantaneous velocity is varied continuously via the stage acceleration profile. The effect of stage acceleration is shown in Fig. 6 for a 4 wt % solution of 50k PS in toluene. Again, the blade height in these experiments was $G=200$ μm and the solution volume was $V=50$ μL. Here, the steepness of the gradient is dictated by the stage acceleration with the slope and thickness range increasing at higher acceleration values. Figure 6(b) reveals that the slope of the gradients ($\Delta h/\Delta d$) exhibits a linear dependence on the acceleration, which is anticipated from the previous results of a linear dependence of film thickness on the stage velocity [see Fig. 4(b)]. At an acceleration of 10 mm s^{-2}, the stage reaches its limiting velocity at $d=32$ mm,[22] and this is reflected in a plateau in the film thickness beyond this distance. Accelerations above 10 mm s^{-2} would lead to steeper gradients, but each gradient would likewise be truncated by the limiting stage velocity of our current instrument.

Alternatively, the thickness gradient can be controlled by varying the solution concentration, as shown in Fig. 7. For this data series, the blade height was $G=200$ μm, the solution volume was $V=50$ μL, and the acceleration of the stage was held constant at $a=6$ mm s^{-2}. Since the velocity profile is linear (as established by a constant acceleration), the gradients in film thickness are linear with respect to position d along the film library. Additionally, the slopes of the gradients increase with increasing solution concentration and exhibit a reasonably linear dependence on con-

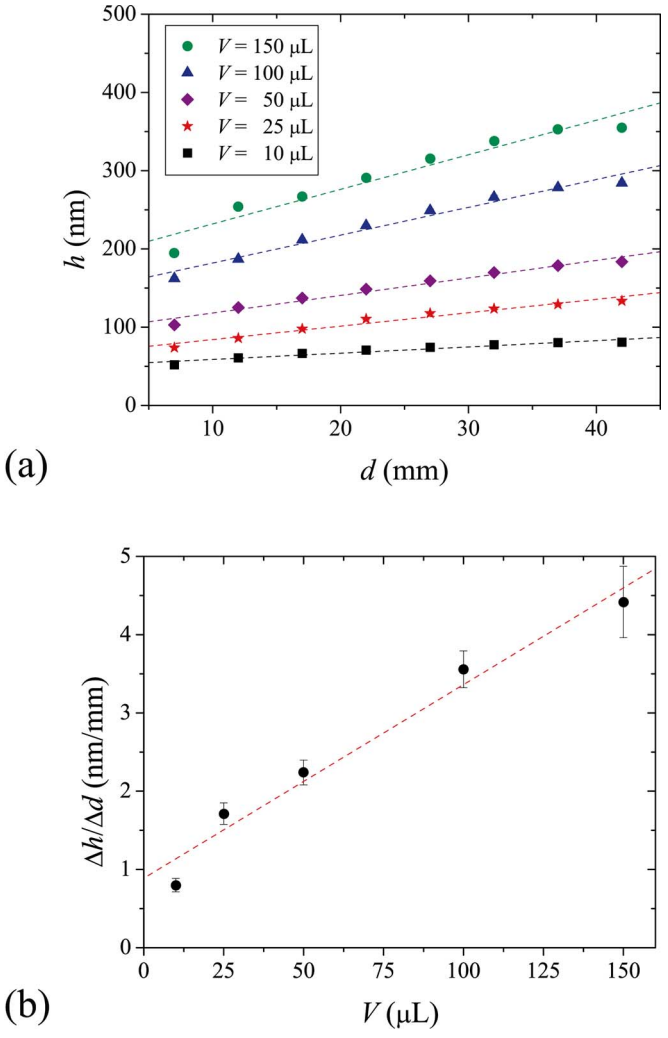

FIG. 8. (Color online) (a) Effect of solution volume (V) on the film thickness gradient (h vs d) for a 4 wt % 50k PS solution in toluene using $a=6$ mm s^{-2} and $G=200$ μm, and (b) the slope of the gradient ($\Delta h/\Delta d$) as a function of solution volume. The dashed lines are linear fits to the data. Most error bars are smaller than the symbols.

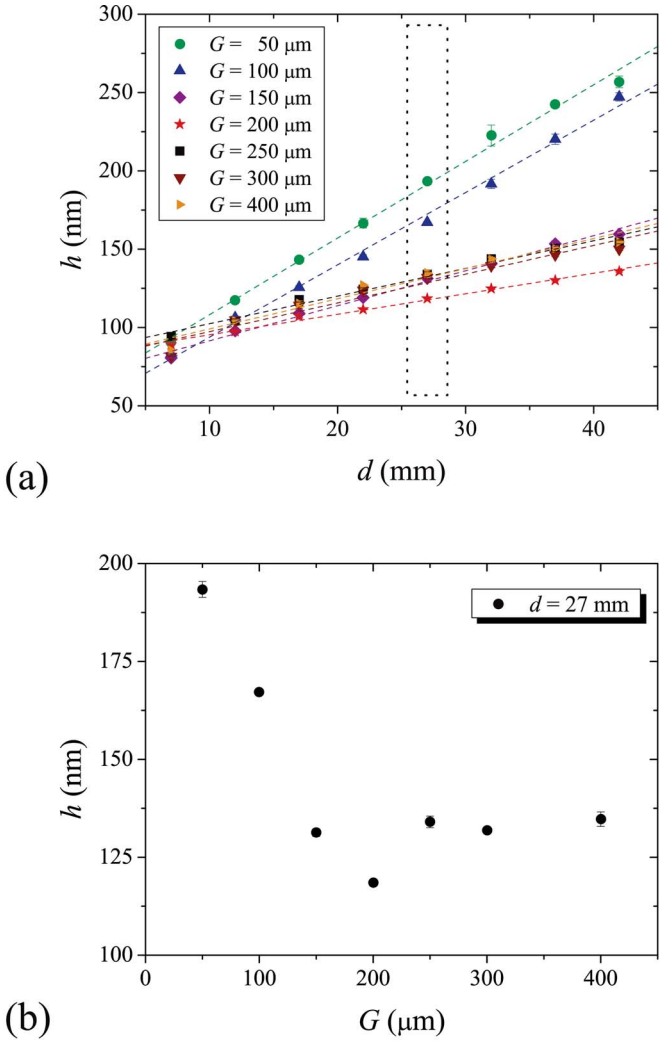

FIG. 9. (Color online) (a) Effect of blade height (G) on the film thickness gradient (h vs d) and (b) a subset of these data at a constant distance, $d=27$ mm [outlined by dotted box in (a)]. The films were prepared from a 3 wt % 50k PS solution using $a=6$ mm s^{-2}, $H=200$ μm, and $V=50$ μL. The dashed lines are linear fits to the data. Most error bars are smaller than the symbols.

centration as shown in Fig. 7(b). Moreover, at an acceleration of 6 mm s^{-2}, the stage reaches its limiting velocity ($v=25$ mm s^{-1}) near the end of the stage travel. Therefore, the maximum thickness at each concentration in Fig. 7 should be equivalent to the constant thickness curves in Fig. 5. An examination of the data confirms that this is indeed true.

We have found that the thickness gradients are also highly dependent on the volume of solution (V) dispensed between the knife blade and substrate. Figure 8 shows thickness gradient data as a function of solution volume, ranging from 10 to 150 μL. The gradients exhibit a systematic increase in slope as the volume of solution under the knife blade increases, with the film thickness exhibiting a reasonably linear dependence on volume of solution dispensed under the blade, as shown in Fig. 8(b).

The effect of the blade gap height (G) on the resulting thickness gradients is shown in Fig. 9. In this example, the films were prepared from a 3 wt % 50k PS solution using $a=6$ mm s^{-2}. The gradients display an interesting dependence on blade gap height, exhibiting a minimum in slope for $G=200$ μm and reaching a plateau for gap heights greater than 200 μm. This is more clearly seen in Fig. 9(b) where the thickness of each film is plotted versus gap height at a fixed distance d of 27 mm, as highlighted by the dotted box in Fig. 9(a). It is important to note that all gap heights explored in this study result in thickness gradients. Combined with the data from Figs. 5–8, a wide range of thickness gradients can be achieved by appropriate combinations of acceleration, concentration, blade height, and solution volume.

Finally, we demonstrate that the flow coating technique is not limited to a particular solvent (e.g., toluene). We prepared identical solutions ($c=30$ mg mL^{-1}) of 50k PS in three organic solvents: toluene, chloroform, and propylene glycol methyl ether acetate (PGMEA). This study also allows us to also explore the effect of solvent quality and volatility on the resulting thickness gradient. One might anticipate that lower vapor pressure solvents might lead to a degradation of the gradient as the wet film could reflow in the time required

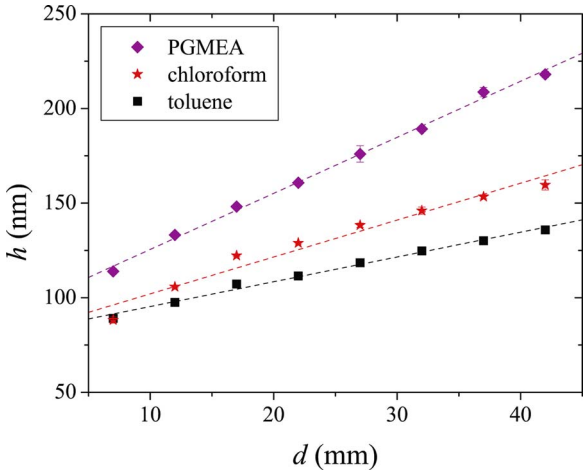

FIG. 10. (Color online) Effect of casting solvent on the film thickness gradient (h vs d) for 30 mg mL^{-1} 50k PS solutions using $a=6$ mm s^{-2}, $G=200$ μm, $V=50$ μL. The dashed lines are linear fits to the data. Most error bars are smaller than the symbols.

for the solvent to evaporate from the film. We chose to prepare these solutions by weight of polymer to volume of solvent due to the large differences in solvent density. The results of flow coating these solutions, with $a=6$ mm s^{-2} and $G=200$ μm, are shown in Fig. 10. When coating from chloroform, the evaporation front appears immediately behind the moving knife blade due to chloroform's high vapor pressure. Toluene evaporates slower, and the evaporation front lags a reasonable distance ($\approx$cm) behind the knife blade. When coating from PGMEA, the entire film remains liquid even after the stage stops, and the evaporation of PGMEA from the wet film occurs over a much longer time scale ($\approx$30 to 60 s). However, the gradient in thickness of the wet film appears to be preserved as indicated by the thickness gradient in the dry film.

ACKNOWLEDGMENTS

Contribution of the National Institute of Standards and Technology is not subject to copyright in the United States. This work was conducted at the NIST Combinatorial Methods Center. One of the authors (K.E.R.) acknowledges the NIST Summer Undergraduate Research Fellowship Program, and one of the authors (T.H.E.) acknowledges the NIST/NRC Postdoctoral Fellowship Program for funding. The authors acknowledge Dr. Wenhua Zhang for programming the computer interface for the flow coater and interferometer.

[1] See, for example, E. M. Gordon, M. A. Gallop, and D. V. Patel, Acc. Chem. Res. **29**, 144 (1996); L. A. Thompson and J. A. Ellman, Chem. Rev. (Washington, D.C.) **96**, 555 (1996) and references therein.
[2] See, for example, I. Takeuchi, J. Lauterbach, and M. J. Fasolka, Mater. Today **8**, 18 (2005); H. E. Tuinstra and C. H. Cummins, Adv. Mater. (Weinheim, Ger.) **12**, 1819 (2000); R. Hoogenboom, M. A. R. Meier, and U. S. Schubert, Macromol. Rapid Commun. **24**, 15 (2003), and references therein.
[3] J. J. Hanak, J. Mater. Sci. **5**, 964 (1970).
[4] J. S. Wang, Y. Yoo, C. Gao, I. Takeuchi, X. D. Sun, H. Y. Chang, X. D. Xiang, and P. G. Shultz, Science **279**, 1712 (1998).
[5] J. C. Meredith, A. Karim, and E. J. Amis, Macromolecules **33**, 5760 (2000).
[6] H. Mao, T. Yang, and P. S. Cremer, J. Am. Chem. Soc. **124**, 4432 (2002).
[7] J. C. Meredith, A. Karim, and E. J. Amis, Mater. Res. Bull. **27**, 330 (2002).
[8] S. V. Roberson, A. J. Fahey, A. Sehgal, and A. Karim, Appl. Surf. Sci. **200**, 150 (2002).
[9] H. Lu, J. W. Stansbury, and C. N. Bowman, J. Dent. Res. **84**, 822 (2005).
[10] J. C. Meredith, A. Karim, and E. J. Amis, Macromolecules **33**, 9747 (2000).
[11] S. Chattopadhyay and J. C. Meredith, Meas. Sci. Technol. **16**, 128 (2005).
[12] A. P. Smith, J. F. Douglas, J. C. Meredith, E. J. Amis, and A. Karim, Phys. Rev. Lett. **87**, 015503 (2001).
[13] A. P. Smith, A. Sehgal, J. F. Douglas, A. Karim, and E. J. Amis, Macromol. Rapid Commun. **24**, 131 (2003).
[14] A. J. Crosby, M. J. Fasolka, and K. L. Beers, Macromolecules **37**, 9968 (2005).
[15] J. Y. Lee and A. J. Crosby, Macromolecules **38**, 9711 (2005).
[16] S. J. Weinstein and K. J. Ruschak, Annu. Rev. Fluid Mech. **36**, 29 (2004).
[17] K. J. Ruschak, Annu. Rev. Fluid Mech. **17**, 65 (1985).
[18] The stage assembly is comprised of Newport Models 37 and 460A, combined with Newport Model 360-90 right-angle brackets.
[19] The x-axis motor is comprised of a computer-controlled translation stage with 50 mm of travel (Parker Automation). The y-axis motor is comprised of a computer-controlled translation stage with 100 mm of travel (Daedal Positioning). Both stages are equipped with Hall-effect limit switches for deenergizing the motors if the motors reach their respective ends of travel.
[20] Equipment and instruments or materials are identified in the paper in order to adequately specify the experimental details. Such identification does not imply recommendation by NIST, nor does it imply the materials are necessarily the best available for the purpose.
[21] In all figures, the error bars represent one standard deviation of the data, which is taken as the experimental uncertainty of the measurement.
[22] This can be calculated by Torricelli's Equation, $v_f^2=v_i^2+2aD$, where we know the highest allowable velocity ($v_f=25$ mm s^{-1}), the initial velocity ($v_i=0$ mm s^{-1}), and the acceleration ($a=6$ mm s^{-2}). Thus, the highest velocity allowable will be reached at $D=52$ mm for an acceleration of 6 mm s^{-2}.